# Beamlike Harmonic Vibration of Variable-Thickness Sandwich Plates

Chu-Ho Lu*
*Memphis State University, Memphis, Tennessee 38152*
and
Charles Libove†
*Syracuse University, Syracuse, New York 13244*

**A theory is presented for the beamlike harmonic vibration of linearly elastic variable-thickness sandwich plates that are symmetrical about a middle surface. In the analysis the face sheets are treated as membranes, the core is assumed to be deformable in transverse shear and to be inextensible in the thickness direction, and all core stresses on cross sections normal to the middle surface are assumed to be negligible, except for the transverse shear. The participation of the face sheet membrane forces in resisting transverse shear by virtue of their inclinations is taken into account. Numerical and experimental results show that neglecting this participation can lead to significant errors if the transverse shear modulus of the core is low and the thickness variation is appreciable.**

## Nomenclature

| | |
|---|---|
| $a$ | = plate length in $x$ direction |
| $D(x)$ | = local flexural stiffness, $=Eth^2/2$ |
| $G(x)$ | = core shear modulus |
| $h(x)$ | = core thickness |
| $I$ | = identity matrix [Eq. (22)] |
| $I(x)$ | = mass moment of inertia per unit of middle-surface area |
| $M(x)$ | = bending moment per unit width |
| $N$ | = number of segments for finite-difference equations |
| $p_1(x), p_2(x)$ | = pressure distributions on upper and lower surfaces, respectively |
| $p(x)$ | = antisymmetric component of pressure loadings, $=\frac{1}{2}[p_1(x)-p_2(x)]$ |
| $Q(x)$ | = transverse shear per unit width |
| $q(x)$ | = running vertical loading |
| $R_1$ | = dimensionless measure of transverse shear flexibility |
| $t(x)$ | = face sheet thickness |
| $w(x)$ | = vertical ($z$-wise) displacement of cross section |
| $x,y,z$ | = coordinates |
| $\beta$ | = thickness taper parameter for plate with linear thickness variation |
| $\Delta$ | = segment length in $x$ direction, $a/N$ |
| $\theta(x)$ | = cross-sectional rotations |
| $\mu(x)$ | = mass per unit area of middle surface, due to core and face sheets combined |
| $\lambda$ | = dimensionless circular frequency |
| $\rho(x)$ | = face sheet radius of curvature |
| $\rho_c, \rho_f$ | = density of core material and face sheet material, respectively |
| $\xi$ | = dimensionless coordinate, $x/a$ |
| $\phi(x)$ | = face sheet sloping angle |
| $\omega$ | = circular frequency |

Received July 5, 1989; revision received Oct. 7, 1990. 

*Visiting Assistant Professor, Mechanical Engineering Department.
†Professor, Department of Mechanical and Aerospace Engineering. Associate Fellow AIAA.

## Introduction

FULL-DEPTH low-density honeycomb is being used in the empennage and control surface elements of aircraft.[1-8] Thus, it is desirable to have a small-deflection theory for the elastic stress analysis of sandwich plates of variable thickness with cores that are deformable in transverse shear. Such a theory is developed in a previous paper[9] and in the present work. Particular reference is made to rectangular plates that are symmetrical about a middle surface, have uniform properties in one direction, and are loaded and supported so that they behave like wide beams in plane-strain bending. Our previous paper[9] dealt with the static analysis of such plates, whereas the present paper deals with their harmonic vibration analysis.

In both cases the face sheets are treated as membranes, the core is assumed to be inextensible in the thickness direction, and all of the core stresses on cross sections normal to the middle surface are assumed to be negligible, except for the transverse shear. The assumptions regarding the core are usually considered to be acceptable for honeycomb or foamed plastic cores.

No restriction is placed on the nature or magnitude of the thickness variation, and the participation of the face sheet membrane forces in resisting transverse shear by virtue of their inclinations is taken into account. One can expect that neglecting this participation (i.e., assuming that the constant-thickness constitutive equations[10] are valid locally, as was done in Ref. 11) may lead to significant errors if the transverse shear modulus of the core is low. This expectation is borne out by the numerical and experimental results to be presented. (Hereafter, variable-thickness sandwich plate analysis based on the assumption that the constant-thickness constitutive equations are valid locally will be referred to as the "simple theory.")

The present analysis is based on the system of four differential equations developed in Ref. 9 for the static analysis of the beamlike bending of variable-thickness sandwich plates [Eqs. (10) and (13–15) of Ref. 9]. These equations will be repeated here for convenience [as Eqs. (2–5)] and then modified to make them applicable to the analysis of harmonic vibration, free or forced, and a simple finite-difference procedure for solving the modified system will be formulated. In the case of free vibration the objective will be to determine the natural frequencies and modes. In the case of forced vibration it will be to determine the response to excitations in the form of prescribed and harmonically varying surface pressures, end

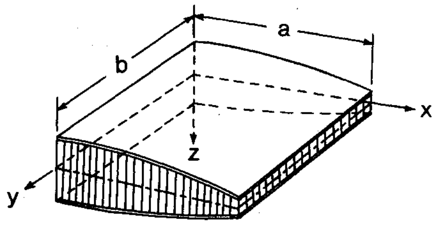


**Fig. 1 Sandwich plate with variation of properties in $x$ direction only and having $x$-$y$ plane as a plane of symmetry.**

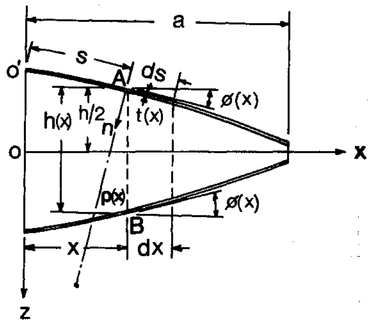


**Fig. 2 Cross section of plate of Fig. 1.**

lateral displacements or shears, and end rotations or bending moments, all in phase.

## Analysis

### Plate Geometry

Figure 1 is an overall view of the plate. The material and geometric parameters and the loading may vary in the $x$ direction, but are uniform in the $y$ direction. The cross-sectional view (Fig. 2) shows the thickness $h$, the face sheet thickness $t(\ll h)$, and face sheet sloping angle $\phi$, all as functions of $x$. Any location $A$ in the upper face sheet is identified by its $x$ coordinate or by its coordinate $s(x)$. The face sheet radius of curvature at $A$ is $\rho(x)$. The variables in Fig. 2 are not all independent, but are related as follows:

$$\frac{\mathrm{d}h}{\mathrm{d}x} = -2\tan\phi \tag{1a}$$

$$\mathrm{d}s = (\sec\phi)\,\mathrm{d}x \tag{1b}$$

$$\frac{1}{\rho} = \frac{\mathrm{d}\phi}{\mathrm{d}s} = \cos\phi\frac{\mathrm{d}\phi}{\mathrm{d}x} \tag{1c}$$

### Loading of Ref. 9

The static loading considered in Ref. 9 is illustrated in Fig. 3. It consists of a running vertical loading $q(x)$ (force per unit of middle-surface area); a running moment $m(x)$ (moment per unit of middle-surface area); end moments $M_0$ and $M_1$, and end shears $Q_0$ and $Q_1$, all per unit width in the $y$ direction; and a pressure $p(x)$ on the upper surface, and a suction of the same magnitude on the lower surface. [The pressure and suction just described actually constitute only the antisymemtric (about the middle surface) component of more general surface loadings. More precisely, $p(x) = ½[p_1(x) - p_2(x)]$, where $p_1(x)$ and $p_2(x)$ are the pressure distributions on the upper and lower surfaces, respectively. The symmetrical component, which has equal pressures of $½[p_1(x)+p_2(x)]$ on both surfaces, will produce no lateral deflections and is therefore not considered.]

### Differential Equations for Static Analysis

Let $M(x)$ be the bending moment per unit width and $Q(x)$ the transverse shear per unit width (Fig. 4). Then, consideration of the infinitesimal element of the beam in Fig. 4 yields the following equations [Eqs. (13) and (14) of Ref. 9] expressing the equilibrium of forces and moments:

$$\frac{\mathrm{d}Q}{\mathrm{d}x} + 2p + q = 0 \tag{2}$$

$$\frac{\mathrm{d}M}{\mathrm{d}x} + Q + m + \frac{1}{2}ph\frac{\mathrm{d}h}{\mathrm{d}x} = 0 \tag{3}$$

Two additional equations are the constitutive equations [Eqs. (10) and (15)] of Ref. 9, namely,

$$M = D\cos^3\phi\left[\frac{\mathrm{d}\theta}{\mathrm{d}x} + \frac{2}{h}\tan\phi\left(\frac{\mathrm{d}w}{\mathrm{d}x} - \theta\right)\right] \tag{4}$$

$$Q = \frac{2M}{h}\tan\phi + Gh\left(\frac{\mathrm{d}w}{\mathrm{d}x} - \theta\right) \tag{5}$$

where $\theta(x)$ and $w(x)$ are, respectively, the rotation (radians, positive clockwise) about the middle surface and the translation (positive downward) of a typical cross section of the plate, $G(x)$ is the local shear modulus of the core for shearing in the $x$-$z$ plane, and $D \equiv Eth^2/2$ with $E(x)$ the local elastic modulus of the face sheets. ($E$ is to be interpreted as the effective modulus, taking into account the suppression of strain in the $y$ direction. However, when the plate is narrow, as in the case of the test specimens to be discussed later, $E$ should be taken as the conventional elastic modulus.)

### Modified Differential Equations

Equations (2-5) are the four equations from Ref. 9 referred to in the Introduction. The following changes are needed in these equations to make them suitable for harmonic vibration analysis: 1) Replace the ordinary derivatives by partial derivatives and regard $Q$, $M$, $w$, $\theta$, and $p$ now as functions of $x$ and of time $t$. 2) Replace $q$ by the lateral inertia loading $-\mu\partial^2 w/\partial t^2$, where $\mu(x)$ is the mass per unit of middle-surface area, due to the core and face sheets combined. 3) Replace $m$

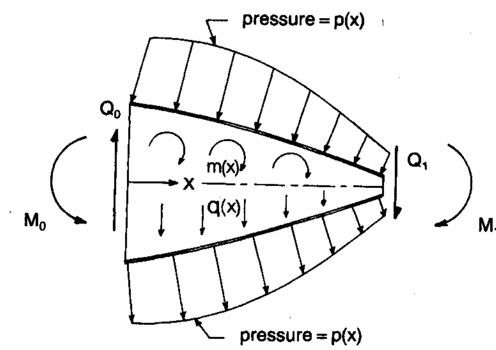


**Fig. 3 Static loading considered in Ref. 9.**

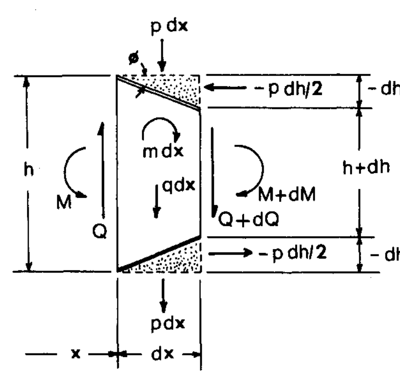


**Fig. 4 Free-body diagram of infinitesimal length of plate under antisymmetric loading.**

by the rotary inertia $-I\partial^2\theta/\partial t^2$, where $I(x)$ is the mass moment of inertia per unit of middle-surface area about the middle surface, due to the core and face sheets combined. For harmonic vibration, $Q$, $w$, $M$, $\theta$, and $p$ can be expressed as

$$Q(x,t) = Q^*(x)\sin\omega t, \qquad w(x,t) = w^*(x)\sin\omega t$$
$$M(x,t) = M^*(x)\sin\omega t, \qquad \theta(x,t) = \theta^*(x)\sin\omega t$$
$$p(x,t) = p^*(x)\sin\omega t \tag{6}$$

where $w$ is the circular frequency. This, plus the use of Eq. (1a) to eliminate $\tan\phi$, reduces Eqs. (2-5) to

$$\frac{dQ}{dx} + 2p + \mu\omega^2 w = 0 \tag{7a}$$

$$\frac{dM}{dx} + Q + I\omega^2\theta + \frac{1}{2}ph\frac{dh}{dx} = 0 \tag{7b}$$

$$M - D\cos^3\phi\left[\frac{d\theta}{dx} - \frac{1}{h}\frac{dh}{dx}\left(\frac{dw}{dx} - \theta\right)\right] = 0 \tag{7c}$$

$$q + \frac{M}{h}\frac{dh}{dx} - Gh\left(\frac{dw}{dx} - \theta\right) = 0 \tag{7d}$$

where, for simplicity, we have omitted the asterisks on the symbols $Q$, $M$, $w$, $\theta$, and $p$, so that henceforth those symbols will represent functions of $x$ alone, not $x$ and $t$. For reduction to the simple theory we may set $\phi$ and $dh/dx$ equal to zero in Eqs. (7).

#### Finite-Difference Form of Modified Differential Equations

Equations (7) are four equations governing the four unknown functions of $x$, namely, $M$, $Q$, $w$, and $\theta$. In a free vibration problem $\omega$ will constitute an additional unknown and $p$ can be dropped, whereas in forced vibration $\omega$ and $p$ will be given. The mathematical problem at this point is to solve the system [Eqs. (7)] for its unknowns, given appropriate boundary conditions. A practical solution to this problem can be effected by the method of finite differences, as shown in the following.

The interval $x = 0$ to $a$ is first divided into $N$ segments of equal length $\Delta = a/N$ by means of $N+1$ stations at $x = 0$, $\Delta$, $2\Delta, \ldots, N\Delta\ (=a)$. Starting from the left end, the segments are numbered, $1, 2, \ldots, N$ and the stations $0, 1, 2, \ldots, N$. Thus, segment $n$ is bounded by stations $n-1$ and $n$. It will also be convenient to let $x_n = n\Delta = na/N$ denote the value of $x$ at station $n$ and to let $\mu_n$, $I_n$, $A_n$, $B_n$, $C_n$, $H_n$, and $p_n$ denote any reasonable approximations to $\mu$, $I$, $h\,dh/dx$, $D\cos^3\phi$, $(1/h)\,dh/dx$, $Gh$, and $p$, respectively, in the segment $n$. Also, the derivatives $dQ/dx$, $dM/dx$, $dw/dx$, and $d\theta/dx$ within the $n$th segment will be replaced by their following constant approximations:

$$\frac{dQ}{dx} = \frac{1}{\Delta}\left[Q(x_n) - Q(x_{n-1})\right] \tag{8a}$$

$$\frac{dM}{dx} = \frac{1}{\Delta}\left[M(x_n) - M(x_{n-1})\right] \tag{8b}$$

$$\frac{dw}{dx} = \frac{1}{\Delta}\left[w(x_n) - w(x_{n-1})\right] \tag{8c}$$

$$\frac{d\theta}{dx} = \frac{1}{\Delta}\left[\theta(x_n) - \theta(x_{n-1})\right] \tag{8d}$$

and $Q(x)$, $M(x)$, $w(x)$, and $\theta(x)$ themselves will be approximated by the following averages of their endpoint values:

$$Q(x) = \left[Q(x_n) + Q(x_{n-1})\right]/2 \tag{9a}$$

$$M(x) = \left[M(x_n) + M(x_{n-1})\right]/2 \tag{9b}$$

$$w(x) = \left[w(x_n) + w(x_{n-1})\right]/2 \tag{9c}$$

$$\theta(x) = \left[\theta(x_n) + \theta(x_{n-1})\right]/2 \tag{9d}$$

As a result of these approximations, Eqs. (7), written for the midpoint of segment $n$, take the following finite-difference form:

$$\frac{1}{\Delta}\left[Q(x_n) - Q(x_{n-1})\right] + 2p_n + \frac{\mu_n\omega^2}{2}\left[w(x_n) + w(x_{n-1})\right] = 0 \tag{10a}$$

$$\frac{1}{\Delta}\left[M(x_n) - M(x_{n-1})\right] + \frac{1}{2}\left[Q(x_n) + Q(x_{n-1})\right] + \frac{I_n\omega^2}{2}\left[\theta(x_n) + \theta(x_{n-1})\right] + \frac{A_n}{2}p_n = 0 \tag{10b}$$

$$\frac{1}{2}\left[M(x_n) + M(x_{n-1})\right] - \frac{B_n}{\Delta}\left[\theta(x_n) - \theta(x_{n-1})\right] - \frac{B_nC_n}{2}\left[\theta(x_n) + \theta(x_{n-1})\right] + \frac{B_nC_n}{\Delta}\left[w(x_n) - w(x_{n-1})\right] = 0 \tag{10c}$$

$$\frac{1}{2}\left[Q(x_n) + Q(x_{n-1})\right] + \frac{C_n}{2}\left[M(x_n) + M(x_{n-1})\right] - \frac{H_n}{\Delta}\left[w(x_n) - w(x_{n-1})\right] + \frac{H_n}{2}\left[\theta(x_n) + \theta(x_{n-1})\right] = 0 \tag{10d}$$

Multiplying Eqs. (10) through by $2\Delta$ and transposing all of the $n-1$ terms to the right side, we obtain the following matrix relationship between the variables at station $n$ and those at station $n-1$:

$$\begin{bmatrix} 2 & 0 & \omega^2\mu_n\Delta & 0 \\ \Delta & 2 & 0 & \omega^2 I_n\Delta \\ 0 & \Delta & 2B_nC_n & -B_n(2+C_n\Delta) \\ \Delta & C_n\Delta & -2H_n & H_n\Delta \end{bmatrix} \begin{bmatrix} Q(x_n) \\ M(x_n) \\ w(x_n) \\ \theta(x_n) \end{bmatrix} + p_n \begin{bmatrix} 4\Delta \\ A_n\Delta \\ 0 \\ 0 \end{bmatrix}$$
$$= \begin{bmatrix} 2 & 0 & -\omega^2\mu_n\Delta & 0 \\ -\Delta & 2 & 0 & -\omega^2 I_n\Delta \\ 0 & -\Delta & 2B_nC_n & -B_n(2-C_n\Delta) \\ -\Delta & -C_n\Delta & -2H_n & -H_n\Delta \end{bmatrix} \begin{bmatrix} Q(x_{n-1}) \\ M(x_{n-1}) \\ w(x_{n-1}) \\ \theta(x_{n-1}) \end{bmatrix} \tag{11}$$

#### Dynamic Transfer Formula

For simplicity let us denote the square matrix on the left side of Eq. (11) by $S_n$, the square matrix on the right by $T_n$, the first and the second column matrices on the left by $Z_n$ and $Y_n$, respectively, and the column matrix on the right by $Z_{n-1}$. Then Eq. (11) may be written as

$$S_nZ_n + p_nY_n = T_nZ_{n-1} \tag{12}$$

where

$$Z_n = K_n Z_{n-1} - L_n \qquad (n = 1, 2, \ldots, N) \tag{13}$$

and where

$$K_n = S_n^{-1} T_n, \qquad L_n = p_n S_n^{-1} Y_n \tag{14}$$

Through repeated application of Eq. (13), starting with $n = 1$, each $Z_n$ can be expressed in terms of $Z_0$. The outcome will have the form

$$Z_n = U_n Z_0 - V_n \qquad (n = 1, 2, \ldots, N) \tag{15}$$

with the $U_n$ and $V_n$ being $4 \times 4$ and $4 \times 1$ matrices, respectively. A recursion formula can be developed for computing the $U_n$ and $V_n$. To develop the formula, we first note, from Eq. (15), that

$$Z_{n-1} = U_{n-1} Z_0 - V_{n-1} \qquad (n = 2, \ldots, N+1) \tag{16}$$

Substitution of Eqs. (15) and (16) into Eq. (13) then gives

$$U_n Z_0 - V_n = (K_n U_{n-1}) Z_0 - (K_n V_{n-1} + L_n) \qquad (n = 2, \ldots, N) \tag{17}$$

from which the recursion formulas are seen to be

$$U_n = K_n U_{n-1}, \qquad V_n = K_n V_{n-1} + L_n \tag{18}$$

To start the recursion process, $U_1$ and $V_1$ must be known. They can be found by writing Eqs. (13) and (15) for $n = 1$ to get

$$Z_1 = K_1 Z_0 - L_1, \qquad Z_1 = U_1 Z_0 - V_1 \tag{19}$$

then comparing the two equations to get

$$U_1 = K_1, \qquad V_1 = L_1 \tag{20}$$

With $U_1$ and $V_1$ known from Eq. (20), repeated application of Eqs. (18), with $n$ successively set equal to 2, 3, ..., $N$, will give $U_2, U_3, \ldots, U_N$ and $V_2, V_3, \ldots, V_N$.

Once $U_N$ and $V_N$ are known, Eq. (15), written for $n = N$, will give the dynamic transfer formula,

$$Z_N = U_N Z_0 - V_N \tag{21}$$

This formula relates the variables $Q$, $M$, $w$, and $\theta$ at the right edge ($x = x_n = a$) to those at the left edge ($x = x_0 = 0$). The pressure amplitudes $p(x)$ are accounted for in the $V_N$ term. For later use it will be convenient to write Eq. (21) in the form

$$\left[U_n \;\vdots\; -I\right]\left[\frac{Z_0}{Z_N}\right] = \left[V_N\right] \tag{22}$$

where $-I$ is the negative of the identity matrix, or, in the more fully expanded form,

$$\begin{bmatrix} U_{11} & U_{12} & U_{13} & U_{14} & -1 & 0 & 0 & 0 \\ U_{21} & U_{22} & U_{23} & U_{24} & 0 & -1 & 0 & 0 \\ U_{31} & U_{32} & U_{33} & U_{34} & 0 & 0 & -1 & 0 \\ U_{41} & U_{42} & U_{43} & U_{44} & 0 & 0 & 0 & -1 \end{bmatrix} \begin{bmatrix} Q(x_0) \\ M(x_0) \\ w(x_0) \\ \theta(x_0) \\ Q(x_N) \\ M(x_N) \\ w(x_N) \\ \theta(x_N) \end{bmatrix} = \begin{bmatrix} V_{N1} \\ V_{N2} \\ V_{N3} \\ V_{N4} \end{bmatrix} \tag{23}$$

where $U_{11}, \ldots, U_{44}$ denote the known elements of the dynamic transfer matrix $U_N$, and $V_{N1}$, $V_{N2}$, $V_{N3}$, and $V_{N4}$ are the four elements of the pressure matrix $V_N$.

**Free Vibration Analysis**

In a free vibration problem the term involving pressure, namely $V_N$, can be dropped from Eq. (21), and as a consequence Eq. (23) becomes

$$\begin{bmatrix} U_{11} & U_{12} & U_{13} & U_{14} & -1 & 0 & 0 & 0 \\ U_{21} & U_{22} & U_{23} & U_{24} & 0 & -1 & 0 & 0 \\ U_{31} & U_{32} & U_{33} & U_{34} & 0 & 0 & -1 & 0 \\ U_{41} & U_{42} & U_{43} & U_{44} & 0 & 0 & 0 & -1 \end{bmatrix} \begin{bmatrix} Q(x_0) \\ M(x_0) \\ w(x_0) \\ \theta(x_0) \\ Q(x_N) \\ M(x_N) \\ w(x_N) \\ \theta(x_N) \end{bmatrix} = \begin{bmatrix} 0 \\ 0 \\ 0 \\ 0 \end{bmatrix} \tag{24}$$

Also, the boundary conditions in a free vibration problem will specify four amplitudes to be null, one from each of the following pairs:

1) Displacement amplitude $w(x_0)$ or force amplitude $Q(x_0)$;
2) Rotation amplitude $\theta(x_0)$ or moment amplitude $M(x_0)$;
3) Displacement amplitude $w(x_N)$ or force amplitude $Q(x_N)$; and
4) Rotation amplitude $\theta(x_N)$ or moment amplitude $M(x_N)$.

The four null amplitudes may be deleted from the column matrix on the left side of Eq. (24), provided that the corresponding columns of the rectangular matrix are struck out. These deletions will reduce the system [Eq. (24)] to four homogeneous linear equations in the four non-null amplitudes. Nontrivial solutions for these amplitudes will exist for the $\omega$ that makes the determinant of the coefficient matrix of those four equations vanish. The $\omega$ defines the natural frequencies.

As an example, let us consider the case of simple support at both edges, for which the null quantities are $M(x_0)$, $w(x_0)$, $M(x_N)$, and $w(x_N)$. Equation (24) becomes

$$\begin{bmatrix} U_{11} & U_{14} & -1 & 0 \\ U_{21} & U_{24} & 0 & 0 \\ U_{31} & U_{34} & 0 & 0 \\ U_{41} & U_{44} & 0 & -1 \end{bmatrix} \begin{bmatrix} Q(x_0) \\ \theta(x_0) \\ Q(x_N) \\ \theta(x_N) \end{bmatrix} = \begin{bmatrix} 0 \\ 0 \\ 0 \\ 0 \end{bmatrix} \tag{25}$$

The determinantal equation defining the natural frequencies is then

$$\begin{vmatrix} U_{11} & U_{14} & -1 & 0 \\ U_{21} & U_{24} & 0 & 0 \\ U_{31} & U_{34} & 0 & 0 \\ U_{41} & U_{44} & 0 & -1 \end{vmatrix} = 0 \quad \text{or} \quad \begin{vmatrix} U_{21} & U_{24} \\ U_{31} & U_{34} \end{vmatrix} = 0 \tag{26}$$

In a similar fashion the frequency equation for a cantilever plate with boundary conditions $w(x_0)=\theta(x_0)=Q(x_N)=M(x_N)=0$ is found to be

$$\begin{vmatrix} U_{11} & U_{12} \\ U_{21} & U_{22} \end{vmatrix} = 0 \tag{27}$$

For the same cantilever with a nondeflecting knife-edge support under the right edge, the boundary condition $Q(x_N)=0$ is replaced by $w(x_N)=0$, and the frequency equation becomes

$$\begin{vmatrix} U_{21} & U_{22} \\ U_{31} & U_{32} \end{vmatrix} = 0 \tag{28}$$

Finally, if both edges are clamped, the boundary conditions $w(x_0)=\theta(x_0)=w(x_N)=\theta(x_N)=0$ lead to the following frequency equation:

$$\begin{vmatrix} U_{31} & U_{32} \\ U_{41} & U_{42} \end{vmatrix} = 0 \tag{29}$$

To find the mode associated with any natural frequency, the first step consists of substituting the corresponding value of $\omega$ into the reduced form of Eqs. (24) and solving those equations for the four amplitudes appearing in them, utilizing any convenient normalization to make the solution unique. All eight of the amplitudes cited earlier (amplitude pairs 1-4) are then known. Therefore, $Z_0$ is known, and Eq. (13) or (15) (with the pressure terms $L_n$ and $V_n$ omitted) can then be used to find $Z_1, Z_2, \ldots, Z_{N-1}$. These define $Q(x_n)$, $M(x_n)$, $w(x_n)$, and $\theta(x_n)$ at all of the interior stations $x_n (n=1, 2, \ldots, N-1)$.

#### Forced Vibration Analysis

In a forced vibration problem the forcing frequency $\omega$ and the pressure amplitudes $p(x)$ are given, as well as four other amplitudes, one from each of the pairs listed earlier. Equation (23) can then be solved for the four remaining amplitudes.

As an example, let us consider a plate simply supported along both edges and excited only by harmonically varying distributed pressures as well as harmonically varying moments applied to the edge $x=x_0=0$ and $x=x_N=a$. In that case the excitation amplitudes at the edges are

$$M(x_0) = M(x_0)^P \tag{30a}$$

$$w(x_0) = w(x_0)^P = 0 \tag{30b}$$

$$M(x_N) = M(x_N)^P \tag{30c}$$

$$w(x_N) = w(x_N)^P = 0 \tag{30d}$$

where the superscript $P$ stands for prescribed. Substituting Eqs. (30) into Eq. (23), and transposing known quantities to the right side, we obtain

$$\begin{bmatrix} U_{11} & U_{14} & -1 & 0 \\ U_{21} & U_{24} & 0 & 0 \\ U_{31} & U_{34} & 0 & 0 \\ U_{41} & U_{44} & 0 & -1 \end{bmatrix} \begin{bmatrix} Q(x_0) \\ \theta(x_0) \\ Q(x_N) \\ \theta(x_N) \end{bmatrix} = \begin{bmatrix} -U_{12}M(x_0)^P + V_{N1} \\ -U_{22}M(x_0)^P + M(x_N)^P + V_{N2} \\ -U_{32}M(x_0)^P + V_{N3} \\ -U_{42}M(x_0)^P + V_{N4} \end{bmatrix} \tag{31}$$

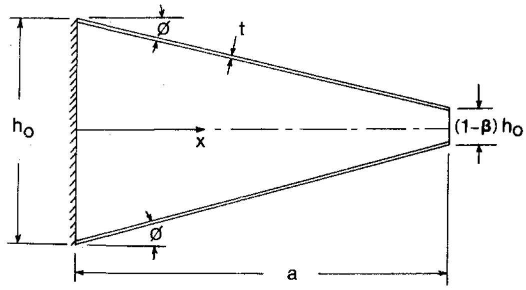


**Fig. 5 Cross section of plate with linear thickness variation.**

and this equation can be solved for the four response amplitudes, $Q(x_0)$, $\theta(x_0)$, $Q(x_N)$, and $\theta(x_N)$.

Once Eq. (31) has been solved, the excitation and response amplitudes at the edges $x=x_0=0$ and $x=x_N=a$ are completely known, and Eq. (13) or (15) can be used to find the response amplitudes $Q(x_n)$, $M(x_n)$, $w(x_n)$, $\theta(x_n)$ at all of the interior stations $x=x_n$ $(n=1, 2, \ldots, N-1)$.

### Illustrative Applications

The analysis in the preceding section will now be demonstrated and its predictions compared with those of the simple theory. For simplicity only free vibration is considered, and only one set of boundary conditions, namely, the boundary condition $w(x_0)=\theta(x_0)=Q(x_N)=M(x_N)=0$ appropriate to a cantilever plate.

#### Description of Plate

In the illustrative applications $E$, $G$, $t$, and $\phi$ will be taken to be independent of $x$. The constancy of $\phi$ implies the linear thickness variation depicted in Fig. 5 and expressible as $h=h_0(1-\beta\xi)$, where $\xi=x/a$, $h_0$ is the thickness at $x=0$, and $\beta$ is a constant quantifying the thickness taper. The variables $\beta$ and $\phi$ are related as follows: $2\tan\phi=-\mathrm{d}h/\mathrm{d}x=\beta h_0/a$. Thus, $D=Eth^2/2=D_0(1-\beta\xi)^2$, where $D_0=Eth_0^2/2$.

To reduce the number of independent variables, we shall approximate $\cos^3\phi$ as 1 and neglect rotary inertia. Then Eqs. (7) can be written in the following dimensionless form:

$$\frac{\mathrm{d}\bar{Q}}{\mathrm{d}\xi} + \lambda^2\bar{w} = 0 \tag{32a}$$

$$\frac{\mathrm{d}\bar{M}}{\mathrm{d}\xi} + \bar{Q} = 0 \tag{32b}$$

$$\bar{M} - B\frac{\mathrm{d}\bar{\theta}}{\mathrm{d}\xi} - BC\bar{\theta} + BC\frac{\mathrm{d}\bar{w}}{\mathrm{d}\xi} = 0 \tag{32c}$$

$$\bar{Q} + C\bar{M} - H\frac{\mathrm{d}\bar{w}}{\mathrm{d}\xi} + H\bar{\theta} = 0 \tag{32d}$$

where $\bar{Q}=Qa^2/D_0$, $\bar{w}=w/a$, $\bar{M}=Ma/D_0$, $\bar{\theta}=\theta$, $\lambda^2=\mu a^4\omega^2/D_0$, $B=(1-\beta\xi)^2$, $C=-\beta/(1-\beta\xi)$, and $H=(1-\beta\xi)/R_1$, with $R_1=D_0/(Gh_0a^2)$. Reducing Eq. (31) to finite-difference form by the same procedure as that used for Eqs. (7), we arrive at Eq. (11) with the pressure term absent, $\Delta$ now equal to $1/N$, bars placed above the symbols $Q$, $M$, $w$, and $\theta$, and $S_n$ and $T_n$ now defined by

$$S_n = \begin{bmatrix} 2 & 0 & \lambda^2\Delta & 0 \\ \Delta & 2 & 0 & 0 \\ 0 & \Delta & 2B_nC_n & -B_n(2+C_n\Delta) \\ \Delta & C_n\Delta & -2H_n & H_n\Delta \end{bmatrix}, \tag{33a}$$

**Table 1 First two dimensionless natural frequencies ($\lambda_1$, $\lambda_2$) for a cantilever plate**

| $R_1$ | $\beta$ | $N = 10$ | $N = 20$ | $N = 40$ | $N = 80$ | Exact |
|---|---|---|---|---|---|---|
| 0.5 | 0 | 1.897 | 1.894 | 1.893 | 1.893 | 1.893 |
| | | 6.020 | 5.934 | 5.913 | 5.908 | 5.906 |
| | 0.5 | 2.037 | 2.033 | 2.032 | 2.032 | |
| | | (1.719) | (1.717) | (1.717) | (1.717) | |
| | | 5.301 | 5.220 | 5.200 | 5.195 | |
| | | (5.221) | (5.145) | (5.126) | (5.121) | |
| | 0.9 | 2.167 | 2.159 | 2.157 | 2.156 | |
| | | (1.510) | (1.508) | (1.508) | (1.508) | |
| | | 4.643 | 4.543 | 4.518 | 4.512 | |
| | | (4.201) | (4.129) | (4.110) | (4.106) | |

Upper value = $\lambda_1$; lower value = $\lambda_2$. Simple theory results in parentheses.

**Table 2 Lowest dimensionless natural frequency ($\lambda_1$) for a cantilever plate with $R_1 \to 0$**

| $\beta$ | $R_1$ | $N = 10$ | $N = 20$ | $N = 40$ | Exact ($R_1 = 0$) |
|---|---|---|---|---|---|
| 0.5 | 0.01 | 3.099 | 3.095 | 3.094 | |
| | | (3.071) | (3.067) | (3.066) | |
| | 0.001 | 3.135 | 3.131 | 3.130 | |
| | 0.0001 | 3.138 | 3.135 | 3.134 | |
| | 0.00001 | 3.139 | 3.135 | 3.134 | |
| | | (3.139) | (3.135) | (3.134) | |
| 0 | 0.00001 | 3.527 | 3.519 | 3.517 | 3.516 |
| | | (3.527) | | | |

(Simple theory results in parentheses.)

$$T_n = \begin{bmatrix} 2 & 0 & -\lambda^2\Delta & 0 \\ -\Delta & 2 & 0 & 0 \\ 0 & -\Delta & 2B_nC_n & -B_n(2-C_n\Delta) \\ -\Delta & -C_n\Delta & -2H_n & -H_n\Delta \end{bmatrix} \tag{33b}$$

where $B_n$, $C_n$, and $H_n$ are the values of $B$, $C$, and $H$, respectively, at the middle of the $n$th segment, i.e., at $\xi = n\Delta - (\Delta/2)$. For reduction to the simple theory we need only replace $B_n$, $C_n$, and $H_n$ in the matrices in Eqs. (33) by 1, 0, and $1/R_1$, respectively.

### Results

For the cantilever plate under consideration, the determinental equation defining the natural frequency parameter $\lambda$ is Eq. (27). The computational procedure for evaluating the required matrix elements $U_{11}$, $U_{12}$, $U_{21}$, and $U_{22}$ associated with any trial value of $\lambda$ is described in detail in the section on the dynamic transfer formula. By this procedure, together with Newton iteration or trial-and-error satisfaction of Eq. (27), the first two values ($\lambda_1$ and $\lambda_2$) of the natural frequency parameter $\lambda$ were obtained for three geometries ($\beta = 0$, 0.5, and 0.9) of a plate with $R_1 = 0.5$. The results are summarized in Table 1, in which, for comparison purpose, a few simple theory results are included in parentheses. For the case $\beta = 0$ "exact" results were obtained by considering the plate to be a wide uniform "Timoshenko beam."

Table 1 indicates that the computed $\lambda$ converge very rapidly as the number of segments $N$ is increased. For all practical purposes complete convergence is obtained with $N = 80$; however, even $N = 10$ gives $\lambda_1$ correct to within 0.5% and $\lambda_2$ to within 2%. The table also shows that the simple theory frequencies (in parentheses) can be appreciably in error.

Because of the presence of $R_1$ as a denominator in the expression for $H$, the computational procedure breaks down when $R_1 = 0$ (infinite transverse shear stiffness). However, this difficulty can be overcome by assigning to $R_1$ a small but nonzero value. Some results obtained in this way for $\lambda_1$ are given in Table 2, which also contains an exact result for the case $\beta = 0$ and some results (in parentheses) corresponding to the simple theory.

Table 2 indicates that, for purpose of calculating $\lambda_1$ with $\beta = 0.5$, $R_1 = 0.01$ is essentially equivalent to $R_1 = 0$. Also, as is to be expected, it shows that, when $R_1$ is very small (negligible transverse shear deformations), the simple theory is quite accurate.

## Experimental Verification

The test specimens were four bilinearly tapered beams of the type shown in Fig. 6. Their tapers were $\beta = 0$, 0.1, 0.3, and 0.5, respectively. The face sheets were of 7075 aluminum alloy 1/32 in. (0.794 mm) thick, 2.32 in. (58.93 mm) wide, and 40.75 in. (1035 mm) long. The elastic modulus and density ($\rho_f$) of this material were $10^7$ psi (68.97 GPa) and 5.420 slug/ft$^3$ (2.793 g/cm$^3$), respectively. They were bonded by means of a mastic adhesive to a rigid foamed plastic core of 0.0322 slug/ft$^3$ (16.6 kg/m$^3$) density ($\rho_c$) and 533 psi (3.68 MPa) shear modulus. The latter value was determined from deflection measurements on the constant-thickness ($\beta = 0$) beam. The mass of the glue per unit of middle-surface area, $m_g$, for the four beams ($\beta = 0$, 0.1, 0.3, and 0.5) were measured as 0.003959 slug/ft$^2$ (0.6217 kg/m$^2$), 0.004318 slug/ft$^2$ (0.6782 kg/m$^2$), 0.004523 slug/ft$^2$ (0.7104 kg/m$^2$), and 0.004934 slug/ft$^2$ (0.7749 kg/m$^2$), respectively.

Based on this data, $\mu(x)$ and $I(x)$ at any location ($x$) of a tapered beam, as shown in Fig. 6, can be approximately evaluated by

$$\mu_n(x) = \rho_c h_i + 2\rho_f t/\cos\phi + m_g \tag{34}$$

$$I_n(x) = \left(\frac{\rho_c}{12}\right) h_i^3 + \rho_f t(h_i + h_f)^2/(8\cos\phi) + m_g\left(\frac{h_i}{2}\right)^2 \tag{35}$$

For $\beta = 0$ the quantities given in Eq. (34) and (35) are constants along the beam given by $\mu = 0.04183$ slug/ft$^2$ (6.569 kg/m$^2$) and $I = 0.0008048$ slug-ft$^2$/ft$^2$ (0.01174 kg-m$^2$/m$^2$).

The devices used were two accelerometers with sensitivity up to 5 kHz, an electromagnetic shaker, two 18-V dc power supplies, a four-channel storage oscilloscope, and a stroboscope that had been calibrated by a tachometer and was accurate to within 0.5%.

The experimental set up is shown in Fig. 7. The specimen is oriented horizontally in the holder, which in turn is fixed on the shaker and subjected to a vertical simple harmonic vibration. The holder is assumed to provide simple support to the ends. Two accelerometers screwed into aluminum blocks are mounted on the specimen: one at the middle of the top face sheet, the other on the upper steel rod of one of the holders. The accelerometer blocks are held in place by means of beeswax. The accelerometers were used to detect the vertical accelerations at their locations. In order to prevent sideways movement of the specimens during vibration, two O-rings are placed on each steel rod of the holder.

The input frequencies were swept from 1 to 140 Hz. Signals sent from the accelerometers went through transducers (i.e., the two 18-V power supplies) and showed two different sinu-

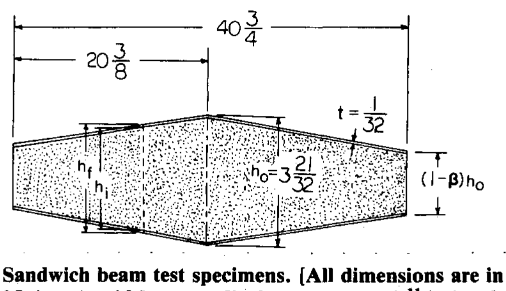


**Fig. 6 Sandwich beam test specimens. [All dimensions are in inches (1 in. = 25.4 mm); width perpendicular to paper = 2 11/32 in.; $h_i$ and $h_f$ are, respectively, the local core thickness and overall thickness; $h_0$ is the value of $h_f$ at the middle.]**

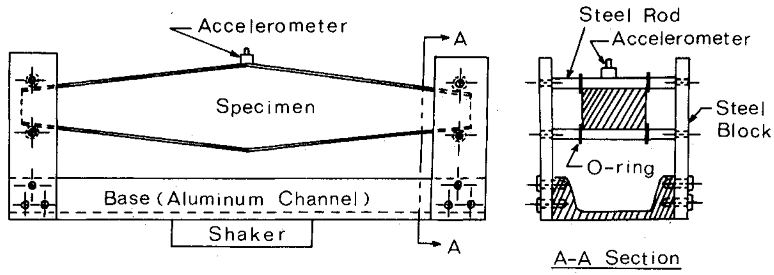


**Fig. 7 Vibration test setup.**

**Table 3 Comparison of theoretical and experimental fundamental frequency, Hz**

| $\beta$ | Experiment | Present theory | Simple theory |
|---|---|---|---|
| 0 | 85.33 | 86.88 | 86.88 |
| 0.1 | 83.17 | 85.65 | 83.95 |
| 0.3 | 82.83 | 83.01 | 77.93 |
| 0.5 | 78.67 | 79.20 | 70.73 |

soidal curves on the oscilloscope screen, indicating the variations of the accelerations at the center of the specimen and the holder. For each input frequency the two accelerometers showed the same output frequency but different amplitudes. The natural frequency was taken as the excitation frequency that gave the maximum ratio of the acceleration response at the center of the specimen to that at the holder. (It was also the excitation frequency at which the responses at the two locations changed from in phase to out of phase.) For the sake of accuracy, excitation frequencies were read from the stroboscope rather than from the control panel dial on the shaker. Since the ends of the specimen are free of moments, and at resonance the vibration amplitude of the holder approaches zero compared to that of the specimen, the assumption of simple support at the ends of the specimen was considered to be justified.

The mass of the midpoint accelerometer, including the aluminum block and the beeswax needed to hold it in place, was about 17% of the mass of the specimen. Therefore, it was not negligible and had to be accounted for in the finite-difference analysis. To that end, the beam was divided into segments, with the concentrated mass $m_c$ constituting segment $n$ of infinitesimal length. For the concentrated mass segment, the equations governing the change of shear, moment, deflection, and rotation were

$$Q_n = Q_{n-1} - \omega^2 m_c w_{n-1}, \qquad w_n = w_{n-1}$$

$$M_n = M_{n-1} - \omega^2 I_c \theta_{n-1}, \qquad \theta_n = \theta_{n-1} \tag{36}$$

where $I_c$ is the rotary inertia of the concentrated mass; however, $I_c$ played no role in the computations, inasmuch as the computation dealt with a symmetrical beam vibrating in a symmetrical mode. Hence, for a beam vibrating in its fundamental mode, $I_c$ can be set equal to zero, and Eqs. (36) reduce to

$$\begin{bmatrix} Q_n \\ M_n \\ w_n \\ \theta_n \end{bmatrix} = \begin{bmatrix} 1 & 0 & -\omega^2 m_c & 0 \\ 0 & 1 & 0 & 0 \\ 0 & 0 & 1 & 0 \\ 0 & 0 & 0 & 1 \end{bmatrix} \begin{bmatrix} Q_{n-1} \\ M_{n-1} \\ w_{n-1} \\ \theta_{n-1} \end{bmatrix} \tag{37}$$

The application of Eq. (11) gives shear, moment, deflection, and rotation at station $n-1$. Using Eq. (37) to compute those quantities due to the effect of the concentrated mass and then applying Eq. (11) again, one is able to get a dynamic transfer matrix relating the variables at the right end ($x = x_N = 2a$) to those at the left end ($x = x_0 = 0$).

By taking 40 segments along each beam, using Eqs. (34) and (35) to approximate the mass and the rotary moment of inertia of each segment, respectively, and taking the mass of the accelerometer into account, we can compute the fundamental frequencies by both the present theory and the simple theory. The calculated frequencies are compared with experiment in Table 3. Again it is seen that the simple theory tends to be increasingly in error as $\beta$ increases, whereas the present theory shows satisfactory agreement with experiment for all of the $\beta$.

## Concluding Remarks

A theory has been presented for the beamlike harmonic vibration of linearly elastic sandwich plates that have thickness variation in one direction, are symmetrical about a middle surface, have cores that are deformable in transverse shear, and have face sheets that can be treated as membranes. The theory takes into account the participation of the face sheet membrane forces in resisting transverse shear by virtue of their inclinations. Its predictions of the natural frequencies of a cantilever plate are compared with those of an alternative theory (simple theory) in which this participation is neglected, and it is shown that the latter theory can be appreciably in error if the shear modulus of the core is low and the thickness taper large. The present theory is also shown to agree with experiment, in contrast to the simple theory.

## Acknowledgment

This material is based upon work supported by National Science Foundation Grant CEE-81-19613.

## References

[1]Mordellet, R. L., "Concorde Elevons: An Exercise in Eutectony," *Proceedings of National SAMPE Technical Conference*, Society of Aerospace Material and Process Engineers, Seattle, WA, Sept. 1969, pp. 141-150.

[2]Saunders, H., and Westerback, S., "Thickness of Adhesive Joints in Sandwich Structures—The Measurement and Acceptance Criteria," *Proceedings of National SAMPE Technical Conference*, Society of Aerospace Material and Process Engineers, Seattle, WA, Sept. 1969, pp. 494-521.

[3]Lansing, W., Dwyer, W., Emerton, R., and Randall, E., "Application of Fully Stressed Design Procedures to Wing and Empennage Structures," *Journal of Aircraft*, Vol. 8, No. 9, 1971, pp. 683-688.

[4]Hayes, R. D., "Application of Advances in Structures and Materials to the Design of the YF-17 Airplane," Society of Automotive Engineers TP-730891, Oct. 1973.

[5]Figge, F. A., and Bernhardt, L., "Air Superiority Fighter Wing Structure Design for Improved Cost, Weight and Integrity," *Journal of Aircraft*, Vol. 12, No. 8, 1975, pp. 670-675.

[6]Bannink, E., Hadcock, R., and Forsch, H., "Advanced Design Composite Material Aircraft Study," *Journal of Aircraft*, Vol. 15, No. 12, 1978, pp. 661-668.

[7]Wetmore, W. C., "Commonality Stressed in New Aircraft," *Aviation Week and Space Technology*, Nov. 12, 1979, pp. 67, 69, 71-74, 79, 81.

[8]Butcher, D. N., "Non-Honeycomb Horizontal Stabilizer," *Astronautics & Aeronautics*, Vol. 19, No. 6, June 1981, p. 50.

[9]Libove, C., and Lu, C.-H., "Beam-Like Bending of Variable-Thickness Sandwich Plates," *AIAA Journal*, Vol. 27, No. 4, 1989, pp. 500-507.

[10]Libove, C., and Batdorf, S. B., "A General Small-Deflection Theory for Flat Sandwich Plates," NACA Rept. 899, 1948.

[11]Huang, S. N., and Alspaugh, D. W., "Minimum Weight Sandwich Beam Design," *AIAA Journal*, Vol. 12, No. 12, 1974, pp. 1617-1618.